

# The crystal structure of jonesite, $\text{Ba}_2(\text{K},\text{Na})[\text{Ti}_2(\text{Si}_5\text{Al})\text{O}_{18}(\text{H}_2\text{O})](\text{H}_2\text{O})_n$ : A first example of titanosilicate with porous double layers

SERGEY V. KRIVOVICHEV<sup>1,\*</sup> AND THOMAS ARMBRUSTER<sup>2</sup>

<sup>1</sup>Institut für Geowissenschaften, Mineralogie/Kristallographie, Kiel Universität, Olshausenstrasse 40, 24118 Kiel Germany

<sup>2</sup>Laboratorium für Chemische and Mineralogische Kristallographie, Universität Bern, Freiestrasse 3, CH-3102 Bern, Switzerland

## ABSTRACT

The crystal structure of jonesite,  $\text{Ba}_2(\text{K},\text{Na})[\text{Ti}_2(\text{Si}_5\text{Al})\text{O}_{18}(\text{H}_2\text{O})](\text{H}_2\text{O})_n$  (monoclinic,  $P2_1/m$ ,  $a = 10.618(2)$ ,  $b = 25.918(4)$ ,  $c = 8.6945(14)$  Å,  $\beta = 127.633(3)^\circ$ ,  $V = 1894.8(6)$  Å<sup>3</sup>,  $Z = 4$ ) from the Benitoite Gem Mine, San Benito County, California has been solved by direct methods from a crystal twinned on (001) and refined to  $R_1 = 0.045$  ( $wR = 0.119$ ,  $S = 1.028$ ) using 3308 unique observed reflections ( $|F_o| \geq 4\sigma_f$ ). The structure is based upon porous double layers of distorted  $\text{Ti}\Phi_6$  octahedra ( $\Phi = \text{O}, \text{H}_2\text{O}$ ) and  $\text{TO}_4$  tetrahedra ( $\text{T} = \text{Si}, \text{Al}$ ) parallel to (010). The layers consist of two sheets of corner-sharing  $\text{Ti}\Phi_6$  octahedra and  $\text{Si}_2\text{O}_7$  groups each. The two adjacent sheets are linked along  $b$  by  $\text{T}_4\text{O}_{12}$  tetrahedral rings that are disordered over two positions. The double layer has an open structure characterized by eight-membered tetrahedral rings with apertures (free diameters) of  $3.37 \times 3.37$  and  $3.33 \times 3.33$  Å<sup>2</sup>, for two symmetrically non-equivalent rings.  $\text{K}^+$  cations and  $\text{H}_2\text{O}$  molecules are located in the pores of the double layers.  $\text{Ba}^{2+}$  cations are between the double layers and provide their linkage into three-dimensional structure. Jonesite is a first example of titanosilicate with porous double-layer structure.

## INTRODUCTION

Within recent few years, titanosilicates and other octahedral-tetrahedral framework materials have attracted considerable attention due to their applications in catalysis, gas separation, energy storage, optoelectronics, radioactive waste management, etc. (Behrens et al. 1998; Lamberti 1999; Rocha and Anderson 2000; Zecchina et al. 2001). Before being synthesized under laboratory conditions, many of these materials were known as minerals. For example, Engelhard titanosilicate ETS-4, which is now used in the gas industry on a multiton scale (Kuznicki et al. 2001), is a synthetic analog of zorite  $[\text{Na}_6\text{Ti}_5(\text{Si}_6\text{O}_{17})_2(\text{O},\text{OH})_5(\text{H}_2\text{O})_{11}]$ , a framework sodium titanosilicate described in the 1970s from alkaline complexes of the Kola peninsula, Russia (Mer'kov et al. 1973; Sandomirskii and Belov 1979). This example and many others show that investigations of minerals not only are of mineralogical interest but also may provide important ideas for synthesis of new materials with important industrial applications.

Jonesite, a rare Ba-K titanosilicate,  $\text{Ba}_2(\text{K},\text{Na})[\text{Ti}_2(\text{Si}_5\text{Al})\text{O}_{18}(\text{H}_2\text{O})](\text{H}_2\text{O})_n$ , was first described by Wise et al. (1977) from the Benitoite Gem mine, San Benito County, California. It occurs in close association with neptunite and joaquinite, and forms crystals up to 1 mm long. However, until now the crystal structure of jonesite could not be solved, despite large crystal size and their relatively good quality.

Wise et al. (1977) pointed out that chemical analysis of jonesite presented a challenging task in its characterization. Even within a single crystal, the composition was variable and bubbling from the sample under the electron beam indicated that it was hydrated. As a consequence, the chemical composition of jonesite was determined by combination of electron microprobe and ion microprobe analyses. The general formula was suggested

as  $(\text{K},\text{Na},\text{Ba})_{1-2}\text{Ba}_4\text{Ti}_4\text{Al}_{1-2}\text{Si}_{10-11}\text{O}_{36}\cdot 6\text{H}_2\text{O}$  taking into account chemical variations resulting from the coupled substitution  $\text{K} + \text{Si} = \text{Ba} + \text{Al}$ . An infrared absorption spectrum obtained by George R. Rossman indicated that water molecules are by far dominant in the mineral in comparison with hydroxyl groups (Wise et al. 1977).

Single-crystal X-ray diffraction (XRD) study performed by Wise et al. (1977) by means of the Weissenberg methods had shown that jonesite is orthorhombic, with space group  $B22_2$  ( $C222_1$  in standard setting), and  $a = 13.730(5)$ ,  $b = 25.904(5)$ ,  $c = 10.608(3)$  Å,  $V = 3773(1.4)$  Å<sup>3</sup>. Inspection of strong spots in the Weissenberg photographs indicated a smaller pseudocell with axes  $a' = a/2 = 6.88$ ,  $b' = b = 25.95$ ,  $c' = c/2 = 5.31$  Å (Wise et al. 1977).

In this paper, we report results of a crystal-structure determination of jonesite.

## EXPERIMENTAL METHODS

The sample of jonesite was obtained from the Excalibur Mineral Company, Peekskill, New York. It contains several rosettes of transparent blades of jonesite on a crossite matrix. The sample originated from the Benitoite Gem mine, San Benito County, California, i.e., the same locality where jonesite was initially described.

A crystal of jonesite selected for data collection was mounted on a Bruker PLATFORM goniometer equipped with an IK SMART CCD detector with a crystal-to-detector distance of 5.4 cm. The data were collected using  $\text{MoK}\alpha$  X-radiation and frame widths of  $0.3^\circ$  in  $\omega$ , with 30 s used to acquire each frame. More than a hemisphere of three-dimensional data was collected. The unit-cell dimensions were refined on the basis of 945 reflections. The data were reduced using the Bruker program SAINT. A semi-empirical absorption-correction based on the intensities of equivalent reflections was applied, and the data were corrected for Lorentz, polarization, and background effects. A total of 10665 intensities was measured; there were 4218 unique reflections with 3308 classified as observed ( $F_o \geq 4\sigma F_o$ ). Scattering curves for neutral atoms, together with anomalous dispersion corrections, were taken from *International Tables for X-Ray Crystallography* (Ibers and Hamilton 1974). The Bruker SHELXTL Version 5.1 system of programs was used for the structure solution and refinement. Initial attempts to solve the structure were made in the space group  $C222_1$  [standard setting of the group  $B22_2$  reported for jonesite by Wise et al. (1977)] with cell dimensions of  $a = 10.618(1)$ ,  $b =$

\*E-mail: skrivovi@mail.ru

**TABLE 1.** Crystallographic data and refinement parameters for jonesite

<i>a</i> (Å)	10.618(2)	Crystal size (mm)	0.24 × 0.18 × 0.01
<i>b</i> (Å)	25.918(4)	Radiation	MoK $\alpha$
<i>c</i> (Å)	8.6945(14)	Total Ref.	10665
$\beta$ (°)	127.633(3)	Unique Ref.	4218
<i>V</i> (Å <sup>3</sup> )	1894.8(6)	Unique $ F_o  \geq 4\sigma_f$	3308
Space group	<i>P</i> <sub>2</sub> / <i>m</i>	<i>R</i> <sub>int</sub>	0.045
<i>F</i> <sub>000</sub>	1693	<i>R</i> <sub>1</sub>	0.045
<i>Z</i>	4	<i>wR</i> <sub>2</sub>	0.119
$\mu$ (cm <sup>-1</sup> )	55.58	<i>S</i>	1.028
<i>D</i> <sub>calc</sub> (g/cm <sup>3</sup> )	3.17		

Notes:  $R_1 = \sum ||F_o| - |F_c|| / \sum |F_o|$ ;  $wR_2 = \{\sum [w(F_o^2 - F_c^2)]^2 / \sum [w(F_o^2)]^2\}^{1/2}$ ;  $w = 1 / [\sigma^2(F_o) + (aP)^2 + bP]$  where  $P = (F_o^2 + 2F_c^2) / 3$ ;  $s = \{\sum [w(F_o^2 - F_c^2)] / (n - p)\}^{1/2}$  where *n* is the number of reflections and *p* is the number of refined parameters.

13.770(3), and *c* = 25.918(6) Å. These attempts were unsuccessful and the cell was transformed into monoclinic primitive one by applying the transformation matrix [100/00 $\bar{1}$ /1/20]. Absence conditions and reflection statistics for the obtained cell (Table 1) were consistent with the space group *P*<sub>2</sub>/*m*. The structure was solved by direct methods in this space group and refined to *R*<sub>1</sub> ~ 0.18. At this stage, a twinning model was introduced into the refinement through the matrix [100/010/ $\bar{1}$ 0 $\bar{1}$ ]. The *R*<sub>1</sub> index immediately dropped to ~ 0.06, with the ratio of two twin components of 0.43/0.57 (more detailed discussion of twinning is given in the Discussion). The final refinement included all atom-position parameters, anisotropic displacement of Ba1, Ba2, Ti1, Ti2, K1, Si1, Si2, Si3, and Si4 atoms, and a weighting scheme of the structure factors. Attempts to refine other Si, K, and O positions anisotropically led to some physically unrealistic displacement parameters. The refinement converged at an agreement index (*R*<sub>1</sub>) of 0.045, calculated for the unique observed reflections, and a goodness-of-fit (*S*) of 1.028. Further details pertinent to data collection and structure refinement are given in Table 1. The final atomic parameters are listed in Table 2, selected interatomic distances are in Table 3. Tables of anisotropic displacement parameters and of observed and calculated structure factors are deposited as Supplementary Information and may also be obtained from the authors upon request.

## RESULTS

### Cation coordination

There are two symmetrically independent Ti sites in the structure of jonesite. Both show very distorted octahedral coordination by five anions. Each Ti $\Phi_6$  octahedron ( $\Phi = O, H_2O$ ) has one short Ti-O bond (1.69–1.72 Å), one long Ti- $\Phi$  bond (2.38–2.41 Å) opposite to the short bond, and four intermediate Ti-O bonds (1.94–2.00 Å). The out-of-center distortions around Ti<sup>4+</sup> cations are 0.374 and 0.355 Å for Ti1 and Ti2, respectively. Such a distortion is typical for octahedrally coordinated *d*<sup>0</sup> transition metals and usually explained on the basis of second-order Jahn-Teller theorem (Kunz and Brown 1995).

There are six main and two additional tetrahedral sites in the structure. The Si1, Si2, Si3, and Si4 sites are occupied solely by Si with the average <Si-O> bond lengths of 1.62, 1.62, 1.61, and 1.62 Å, respectively. The Si5 and Si6 sites are 79%-occupied by equal proportions of Si and Al, which is reflected in the average <Si-O> bond lengths of 1.69 Å for both sites. The Si5A and Si6A sites are only 21% occupied, however. These sites are complementary to the Si5 and Si6 sites and their disorder will be discussed below.

The Ba1 and Ba2 atoms are coordinated by nine and ten O atoms, respectively, with Ba-O bond lengths in the range of 2.704–3.071 Å. There are three K sites in the structure and these are occupied by K and Na in different proportions. The occupancies of the K sites were fixed during refinement in order to be in approximate agreement with the variations in chemical composition of jonesite reported by Wise et al. (1977) and to be consistent with the observed K- $\Phi$  bond lengths to interstitial H<sub>2</sub>O molecules.

**TABLE 2.** Atomic coordinates and isotropic displacement parameters (Å<sup>2</sup>) for jonesite

Atom	Occupancy	<i>x</i>	<i>y</i>	<i>z</i>	<i>U</i> <sub>eq</sub>
Ba1	Ba	0.49799(7)	0.517595(15)	0.24430(6)	0.01207(14)
Ba2	Ba	0.00154(7)	0.47576(2)	-0.24868(7)	0.01449(14)
Ti1	Ti	0.2682(2)	0.57478(6)	-0.2123(2)	0.0121(3)
Ti2	Ti	0.2604(2)	0.43091(6)	0.2752(2)	0.0128(3)
Si1	Si	0.8767(4)	0.60395(9)	0.4844(3)	0.0107(5)
Si2	Si	0.3469(4)	0.38986(9)	-0.0279(3)	0.0146(6)
Si3	Si	-0.1248(3)	0.38956(9)	-0.0289(3)	0.0085(5)
Si4	Si	0.6392(4)	0.39499(8)	0.5151(3)	0.0110(5)
K1	K <sub>0.70</sub> Na <sub>0.30</sub>	0.2822(5)	0.2500	-0.2510(4)	0.049(2)
K2	K <sub>0.50</sub> Na <sub>0.10</sub>	0.7146(6)	0.2500	0.7472(7)	0.027(2)
K3	K <sub>0.40</sub>	0.7884(39)	0.2500	0.7294(36)	0.147(14)
Si5	Si <sub>0.395</sub> Al <sub>0.395</sub>	0.3978(4)	0.31321(14)	0.2522(6)	0.0127(6)
Si6	Si <sub>0.395</sub> Al <sub>0.395</sub>	0.1075(4)	0.31288(12)	0.2618(5)	0.0082(6)
Si5A	Si <sub>0.105</sub> Al <sub>0.105</sub>	0.6085(15)	0.3115(5)	0.2516(20)	0.010*
Si6A	Si <sub>0.105</sub> Al <sub>0.105</sub>	-0.1106(15)	0.3130(5)	0.2263(19)	0.010*
O1	O	0.0389(7)	0.5708(2)	0.5886(9)	0.0190(14)
O2	O	0.7016(7)	0.4275(2)	0.4129(9)	0.0170(14)
O3	O	0.1938(7)	0.3924(2)	-0.2584(8)	0.0185(15)
O4	O	0.7971(7)	0.3896(3)	0.7423(8)	0.021(2)
O5	O	0.2928(7)	0.4247(2)	0.0767(8)	0.0140(13)
O6	O <sub>0.75</sub> (H <sub>2</sub> O) <sub>0.25</sub>	0.2639(7)	0.3382(2)	0.2754(7)	0.0204(12)
O6O7	(H <sub>2</sub> O) <sub>0.79</sub>	0.7684(14)	0.3346(3)	0.2853(10)	0.028(2)
O7A	O <sub>0.21</sub>	0.7375(41)	0.3350(9)	0.2119(37)	0.010*
O8	O <sub>0.79</sub>	0.5782(10)	0.3377(2)	0.4279(9)	0.0060(15)
O8A	O <sub>0.21</sub>	0.6326(34)	0.3306(11)	0.4396(40)	0.010*
O9	O	0.9123(9)	0.6623(2)	0.5668(8)	0.0260(13)
O10	O	0.0265(7)	0.4274(2)	0.0767(9)	0.0163(14)
O11	O	0.2874(7)	0.5099(2)	-0.1701(8)	0.0212(11)
O12	O	0.5023(7)	0.4084(2)	0.0088(8)	0.0210(14)
O13	O	-0.2466(8)	0.4081(3)	0.0079(9)	0.033(2)
O14	O <sub>0.79</sub>	0.3521(10)	0.3286(3)	0.0357(11)	0.018(2)
O14A	O <sub>0.21</sub>	0.4339(31)	0.3349(8)	0.0531(39)	0.010*
O15	O <sub>0.79</sub>	-0.0603(9)	0.3296(3)	0.0429(12)	0.011(2)
O15A	O <sub>0.21</sub>	-0.0970(39)	0.3352(10)	0.0616(39)	0.010*
O16	O	0.4929(7)	0.4239(2)	0.4839(9)	0.0201(14)
O17	O	0.7585(7)	0.5739(2)	0.5114(10)	0.023(2)
O18	O	0.2568(6)	0.4970(3)	0.2743(7)	0.0278(14)
O19	O <sub>0.79</sub>	0.4074(12)	0.2500	0.2796(15)	0.013(2)
O19A	O <sub>0.21</sub>	0.5727(42)	0.2500	0.1993(51)	0.010*
O20	O <sub>0.79</sub>	0.1147(14)	0.2500	0.2868(17)	0.023(3)
O20A	O <sub>0.21</sub>	-0.0981(43)	0.2500	0.2655(50)	0.010*
O21	(H <sub>2</sub> O) <sub>0.72</sub>	0.4920(13)	0.3247(3)	-0.2570(11)	0.043(3)
H <sub>2</sub> O22	(H <sub>2</sub> O) <sub>0.26</sub>	0.5011(50)	0.2500	-0.2472(44)	0.040*
H <sub>2</sub> O23	(H <sub>2</sub> O) <sub>0.40</sub>	0.6266(27)	0.2500	0.0420(31)	0.040*
H <sub>2</sub> O24	(H <sub>2</sub> O) <sub>0.28</sub>	0.9570(27)	0.2820(9)	0.7019(33)	0.040*
H <sub>2</sub> O25	(H <sub>2</sub> O) <sub>0.36</sub>	0.7256(40)	0.2500	-0.0068(46)	0.066(14)

Note: *U*<sub>eq</sub> is defined as one third of the trace of the orthogonalized *U*<sub>*i*</sub> tensor. \* Fixed during refinement.

### Bond-valence analysis

Bond-valence calculations were performed using bond-valence parameters for the Ti<sup>4+</sup>-O, Si<sup>4+</sup>-O, Ba<sup>2+</sup>-O, and K<sup>+</sup>-O taken from Brown and Altermatt (1985). Bond-valence sums for the Ti1, Ti2, Ba1, Ba2, K1, K2, and K3 sites are 4.19, 4.09, 2.02, 1.74, 0.67, 0.58, and 0.58 v.u. (valence units), respectively (not taking into consideration short K-H<sub>2</sub>O bonds (>2.5 Å) that probably correspond to the occupation of the K sites by Na). Bond-valence sums for tetrahedral sites are 4.07, 4.08, 4.08, 4.06, 3.50, 3.28, 3.70, and 3.38 for Si1, Si2, Si3, Si4, Si5, Si6, Si5A, and Si6A, respectively. The low bond-valence sums observed for the Si5, Si6, Si5A, and Si6A sites are in good agreement with their half-half occupancy by Si and Al. Bond-valence sums for O atoms are in the range of 1.80–2.10 v.u., whereas bond-valence sums for H<sub>2</sub>O sites range from 0.06 to 0.40 v.u. The bond valence analysis indicates that there are no hydroxyl groups present in the structure of jonesite, which agrees well with the conclusions of Wise et al. (1977) made on the basis of an IR absorption spectrum of the mineral.

**TABLE 3.** Selected bond lengths (Å) in the structure of jonesite

Ba1-O17	2.708(6)	Si4-O16	1.592(7)
Ba1-O16	2.759(6)	Si4-O8	1.612(7)
Ba1-O18	2.780(6)	Si4-O2	1.630(6)
Ba1-O11	2.813(6)	Si4-O4	1.640(6)
Ba1-O11	2.861(5)	<Si4-O>	1.62
Ba1-O2	2.899(6)		
Ba1-O13	2.914(7)	Si5-O19	1.650(4)
Ba1-O12	2.917(6)	Si5-O14	1.680(9)
Ba1-O5	2.964(6)	Si5-O6	1.683(7)
<Ba1-O>	2.85	Si5-O8	1.683(8)
		<Si5-O>	1.67
Ba2-O18	2.707(6)		
Ba2-O11	2.816(6)	Si6-O20	1.640(3)
Ba2-O5	2.938(5)	Si6-O15	1.687(9)
Ba2-O10	2.955(6)	Si6-O6	1.722(7)
Ba2-O1	2.970(6)	Si6-O9	1.748(8)
Ba2-O1	2.985(6)	<Si6-O>	1.70
Ba2-O2	2.987(6)		
Ba2-O3	3.008(6)	Si5A-O8A	1.57(3)
Ba2-O10	3.029(6)	Si5A-O19A	1.64(2)
Ba2-O4	3.082(7)	Si5A-O14A	1.70(3)
<Ba2-O>	2.95	Si5A-O7A	1.72(4)
		<Si5A-O>	1.66
Ti1-O11	1.706(5)		
Ti1-O1	1.946(6)	Si6A-O15A	1.63(3)
Ti1-O2	1.957(6)	Si6A-O7A	1.64(4)
Ti1-O13	1.977(7)	Si6A-O20A	1.66(1)
Ti1-O12	1.998(6)	Si6A-O9	1.86(1)
Ti1-H <sub>2</sub> O7	2.401(8)	<Si6A-O>	1.70
<Ti1-Φ>	2.00		
		K1-H <sub>2</sub> O22	2.30(5)
		K1-H <sub>2</sub> O23	2.91(2)
Ti2-O18	1.713(7)	K1-O14	2.943(8) 2×
Ti2-O5	1.962(6)	K1-H <sub>2</sub> O21	2.98(1) 2×
Ti2-O10	1.980(6)	K1-O9	3.169(6) 2×
Ti2-O16	1.987(6)	<K1-Φ>	2.92
Ti2-O17	1.988(6)		
Ti2-O6	2.404(6)	K2-H <sub>2</sub> O25	2.07(3)
<Ti2-O>	2.01	K2-H <sub>2</sub> O22	2.30(5)
		K2-H <sub>2</sub> O24	2.95(2) 2×
Si1-O17	1.611(6)	K2-O15	3.013(9) 2×
Si1-O9	1.618(6)	K2-H <sub>2</sub> O21	3.04(1) 2×
Si1-O1	1.619(6)	<K2-Φ>	2.80
Si1-O3	1.623(6)		
<Si1-O>	1.62	K3-H <sub>2</sub> O24	2.12(4) 2×
		K3-H <sub>2</sub> O25	2.75(5)
Si2-O12	1.553(6)	K3-O15	2.99(1) 2×
Si2-O5	1.616(6)	K3-O8	3.14(2) 2×
Si2-O3	1.639(5)	K3-H <sub>2</sub> O22	3.18(6)
Si2-O14	1.670(8)	<K3-Φ>	2.80
<Si2-O>	1.62		
Si3-O13	1.585(7)		
Si3-O10	1.607(6)		
Si3-O4	1.622(6)		
Si3-O15	1.658(8)		
<Si3-O>	1.62		

\* Φ = O, H<sub>2</sub>O.

### Structure description

A projection of the jonesite structure along the *a* axis is shown in Figure 1a. The structure is based on porous double layers of TiΦ<sub>6</sub> octahedra and SiO<sub>4</sub> tetrahedra parallel to (010). The layer consists of two sheets of corner-sharing TiΦ<sub>6</sub> octahedra and Si<sub>2</sub>O<sub>7</sub> groups (Fig. 1b). The Si<sub>2</sub>O<sub>7</sub> groups within the sheets are formed by the Si1, Si2, Si3, and Si4 atoms. The two adjacent sheets are linked along *b* by four-membered T<sub>4</sub>O<sub>12</sub> tetrahedral rings formed by Si5 and Si6 atoms (Fig. 1c). During the refinement, it was observed that the Si5 and Si6 sites are not fully occupied and that the difference Fourier map contained two additional peaks. The positions of these peaks corresponded approximately to the positions of Si5 and Si6 if they were translated by *a*/2 (Fig. 1c).

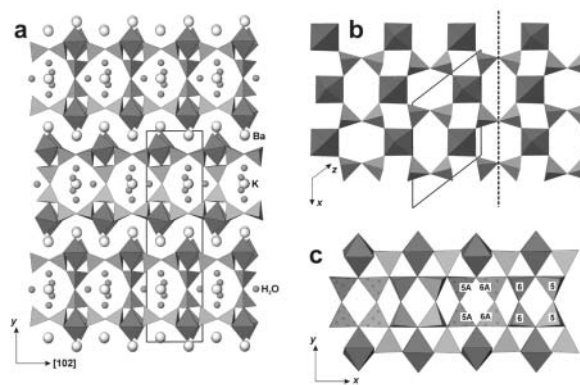


**FIGURE 1.** Crystal structure of jonesite: (a) projection along the *a* axis showing the titanosilicate layers parallel to (010) with pores filled with (K,Na) and H<sub>2</sub>O, linked by Ba; (b) sheet of corner-sharing TiΦ<sub>6</sub> octahedra and Si<sub>2</sub>O<sub>7</sub> groups with twinning plane (001) shown as a dashed line; (c) the arrangement of the Si5-Si6 and Si5A-Si6A 4Rs in the (001) plane.

These positions were introduced into the refinement as Si5A and Si6A and the refinement resulted in ~79% occupancy for the Si5 and Si6 sites and ~21% occupancy for the Si5A and Si6A sites. Thus, the four-membered tetrahedral rings are disordered over two positions related by  $\pm a/2$  (Fig. 1c). The four-membered rings (4R) formed by Si5A and Si6A are located between two translationally equivalent 4Rs formed by Si5 and Si6 atoms, and play the same topological function of linkage of two adjacent sheets into double porous layer. Note that incorporation of 4Rs formed by Si5A and Si6A involves rotation of Si<sub>2</sub>O<sub>7</sub> groups (Fig. 1c).

The titanosilicate layers have an open structure with large channels confined by eight-membered tetrahedral rings (8R) formed as a result of condensation of Si<sub>2</sub>O<sub>7</sub> groups with T<sub>4</sub>O<sub>12</sub> four-membered rings. There are two symmetrically independent 8Rs in the structure: one formed by the Si3, Si4, Si5, and Si6 atoms, and the other formed by Si1, Si2, Si5, and Si6 atoms. The apertures (free diameters) of the eight-membered rings are  $3.37 \times 3.37$  and  $3.33 \times 3.33$  Å<sup>2</sup>, respectively, calculated as a distance between O atoms across the ring *minus* 2.7 Å (two oxygen radii) (Fig. 2). The K and H<sub>2</sub>O21, H<sub>2</sub>O22, H<sub>2</sub>O23, and H<sub>2</sub>O24 sites are within the channels of the layer.

The layers are stacked along the *b* axis as shown in Figure 1a. It should be noted that the disorder of 4Rs observed in the structure may be explained as due to the presence of stacking faults as the double titanosilicate layer can exist in two configurations related by the  $\pm a/2$  translation.

The Ba<sup>2+</sup> cations are located between the layers and provide their linkage into a three-dimensional structure.

### Structural formula

On the basis of the results of crystal-structure solution and refinement, the structural formula of jonesite can be written as Ba<sub>2</sub>(K,Na)[Ti<sub>2</sub>(Si<sub>5</sub>Al)O<sub>18</sub>(H<sub>2</sub>O)](H<sub>2</sub>O)<sub>*n*</sub>, where *n* ~ 1.28 for the crystal studied. This formula is in good agreement with the results of chemical analyses reported for jonesite by Wise et al. (1977). It is clear that the chemical variations observed for jonesite crystals are due to the possibility of Si-Al, Ba-K, and K-Na substitutions. These variations are typical for natural titanosilicates with open

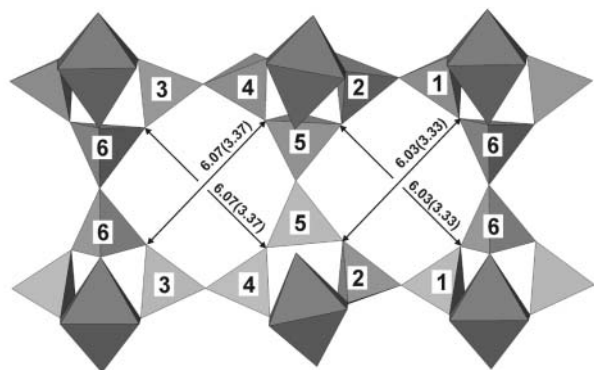


FIGURE 2. Two adjacent eight-membered rings of  $\text{SiO}_4$  tetrahedra and their free diameters (calculated as the distance between O atoms across the ring minus 2.7 Å).

frameworks and, as a result, several mineral species are usually known for a given structure type [e.g., in labuntsovite-nenadkevichite group of minerals (Chukanov et al. 2002)].

## DISCUSSION

### Topological structure of titanosilicate sheet

The topological structure of the titanosilicate layer observed in jonesite can be described using a graphical approach. The Ti octahedra and Si tetrahedra are symbolized by black and white circles, respectively, and their corner linkage is symbolized by a single line. An octahedral-tetrahedral unit is thus associated with a black-and-white graph symbolizing polyhedral connectivity of the unit. For instance, the octahedral-tetrahedral sheet shown in Figure 1b corresponds to a graph depicted in Figure 3a. The graph corresponding to the whole titanosilicate layer in jonesite is shown in Figure 3b. It can be considered as composed of two types of cages shown in Figures 3c and d. Face symbols of these cages are  $8^46^64^43^8$  and  $4^23^2$ , respectively (Liebau 2003) (a face symbol gives number of vertices in a face with the number of such faces given as a superscript).

The  $8^46^64^43^8$  cages have eight-membered rings as windows with the effective pore size of  $3.37 \times 3.37 \text{ \AA}^2$  (see above). The adjacent cages link through 8Rs so that a two-dimensional channel system is formed with channels running parallel to  $[100]$  and  $[001]$ .

### Twinning

As mentioned above, the crystal of jonesite used in this study was twinned on the (001) plane. The twinning model was introduced into the refinement through the matrix  $[100/010/\bar{1}0\bar{1}]$ . The given monoclinic primitive cell [ $a = 10.618(2)$ ,  $b = 25.918(4)$ ,  $c = 8.6945(14) \text{ \AA}$ ,  $\beta = 127.633(3)^\circ$ ] may be transformed into another primitive monoclinic cell with smaller  $\beta$  angle by applying the matrix  $[10\bar{1}/010/\bar{1}0\bar{1}]$ . The resulting cell has  $a' = c' = 8.694$ ,  $b' = 25.918 \text{ \AA}$ ,  $\beta' = 104.73^\circ$  (Fig. 4). As  $a = c$ , this monoclinic cell has a pseudo-mirror plane parallel to  $(10\bar{1})$  and this plane becomes a twin composition plane. In this setting, the twinning matrix is  $[001/010/100]$ , i.e., it corresponds to the interchange of the  $a'$  and  $c'$  axes (Fig. 4). The lattice metric symmetry (geometry)

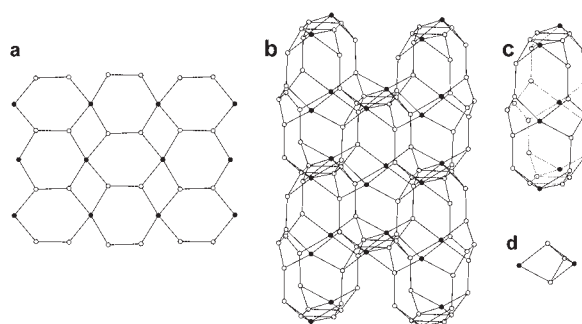


FIGURE 3. Graphical representation of the topology of the titanosilicate layer of jonesite, where the open circles represent tetrahedral sites and closed circles, octahedral sites, which are connected with bonds without O atom bridges. (a) the topology of the sheet of  $\text{TiO}_6$  octahedra and  $\text{Si}_2\text{O}_7$  groups (Fig. 1b). (b) The topology of the double porous layers. (c) and (d) Two types of cages,  $8^46^64^43^8$  and  $4^23^2$ , respectively.

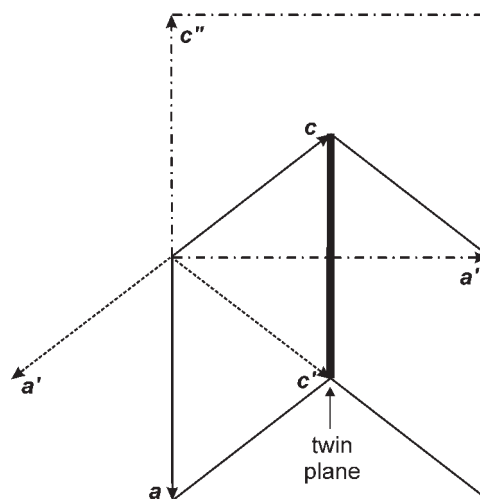


FIGURE 4. Scheme of unit-cell transformations and twinning in the structure of jonesite. Legend:  $a$  and  $c$ , single line: monoclinic cell with  $\beta$  angle of  $127.6^\circ$ ;  $a'$  and  $c'$ , dashed line: monoclinic cell with  $a' = c'$  and  $\beta$  angle of  $104.7^\circ$ ;  $a''$  and  $c''$ , dashed-and-dot line: pseudo-orthorhombic  $B$  supercell. Twin composition plane is parallel to  $(001)$  in the cell with axes  $a$  and  $c$  and to  $(10\bar{1})$  in the cell with axes  $a'$  and  $c'$ .

of jonesite is orthorhombic and is higher than the symmetry of the structure, which is monoclinic. This feature favors twinning of monoclinic structure that emulates orthorhombic symmetry (dashed-and-dot line in Fig. 4; axes  $a''$  and  $c''$ ). This kind of twinning was recently considered by Nespolo and Ferraris (2000) and was called twinning by "metric merohedry."

### Comparison with related structures

Jonesite is the first example of a titanosilicate with a structure based on porous double layers. It is closely related to the titanio-, niobio-, and zirconosilicate minerals whose structures are based on frameworks of corner-sharing octahedra and tetrahedra. More than 30 topologically different frameworks are known in this family, and their detailed description and classification will be

given in a separate paper.

It is of interest that jonesite also is related to modular Ti heterophyllosilicates that recently attracted considerable attention due to interesting polysomatic relationships (Ferraris 1997). The octahedral-tetrahedral sheet shown in Figure 1b has been observed in several minerals, e.g., in bafertisite (Guan et al. 1963) and lomonosovite (Rastsvetaeva et al. 1986). Replacement of  $Ti\Phi_6$  octahedron in this sheet by  $Ti\Phi_5$  tetragonal pyramid results in the heteropolyhedral sheet observed in lamprophyllite polytypes (Krivovichev et al. 2003b). However, in these Ti heterophyllosilicates, adjacent sheets are linked by intermediate brucite-like octahedral sheets into three-level layers that are separated in the structure by alkali metal or alkali earth cations such as  $K^+$ ,  $Ba^{2+}$ , and  $Sr^{2+}$ . In contrast, in jonesite, adjacent octahedral-tetrahedral sheets are linked by four-membered tetrahedral rings that produce layers with internal channels occupied by  $H_2O$  molecules and weak cations such as  $K^+$  and  $Na^+$ .

Recently, Liebau (2003) suggested a new system of classification of poroates (= ordered macroporous and mesoporous materials with inorganic hosts). According to this system, jonesite should be considered as poroate-[4,6], which reflects construction of its porous part from cations in tetrahedral (4) and octahedral (6) coordinations. The host is two-dimensional ( $D^h = 2$ ), and can be considered as based upon cages (**K**) as fundamental building units (**FBU**). Among poroates-[4], a similar structure is observed for rhodesite, a double-layer silicate of the idealized composition  $HKC a_2[Si_8O_{19}](6x)H_2O$  (Hesse et al. 1992), and minerals of the tobermorite group (Merlino et al. 1999, 2001). Their structures consist of porous tetrahedral double layers (rhodesite) or double chains (tobermorite) interlinked via sheets of Ca polyhedra. Cations and  $H_2O$  molecules are in the eight-membered ring channels.

#### ACKNOWLEDGMENTS

The manuscript was essentially improved following reviews of Giovanni Ferraris and William S. Wise, and comments of Associate Editor Simona Quartieri. We thank Friedrich Liebau for calling our attention to the jonesite problem. S.V.K. thanks Alexander von Humboldt foundation for the European research fellowship and the Swiss National Foundation for support during stay at Bern (grant no. 20-65084.01 to T.A., Crystal chemistry of minerals).

#### REFERENCES CITED

- Behrens, E.A., Sylvester, P., and Clearfield, A. (1998) Assessment of a sodium nonatitanate and pharmacosiderite-type ion exchanger for strontium and cesium removal from DOE waste simulants. *Environmental Science and Technology*, 32, 101–107.
- Brown, I.D. and Altermatt, D. (1985) Bond-valence parameters obtained from a systematic analysis of the Inorganic Crystal Structure Database. *Acta Crystallographica*, B41, 244–247.
- Chukanov, N.V., Pekov, I.V., and Khomyakov, A.P. (2002) Recommended nomenclature for labuntsovite-group minerals. *European Journal of Mineralogy*, 14, 165–174.
- Ferraris, G. (1997) Polysomatism as a tool for correlating properties and structure. *EMU Notes in Mineralogy*, 1, 275–295.
- Guan, Ya.S., Simonov, V.I., and Belov, N.V. (1963) Crystal structure of bafertisite,  $BaFe_2TiO[Si_2O_7](OH)_2$ . *Doklady Akademii Nauk*, 149, 1416–1419.
- Hesse, K.F., Liebau, F., and Merlino, S. (1992) Crystal structure of rhodesite,  $HK_{1-x}Na_{x+2y}Ca_{2-y}(IB,3,2\infty)(Si_8O_{19})^{-(6-z)}H_2O$ , from three localities and its relation to other silicates with dreier double layers. *Zeitschrift für Kristallographie*, 199, 25–48.
- Ibers, J.A. and Hamilton, W.C., Eds. (1974) *International Tables for X-ray Crystallography*. Vol. IV. The Kynoch Press, Birmingham, U.K.
- Krivovichev, S.V., Yakovenchuk, V.N., Burns, P.C., Pakhomovsky, Ya.A., Men'shikov, Yu.P. (2003a) Cafetite,  $Ca[Ti_2O_3](H_2O)$ : crystal structure and revision of chemical formula. *American Mineralogist*, 88, 424–429.
- Krivovichev, S.V., Armbuster, T., Yakovenchuk, V.N., Pakhomovsky, Ya.A., and Men'shikov, Yu.P. (2003b) Crystal structures of lamprophyllite-2M and lamprophyllite-2O from the Lovozero alkaline massif, Kola peninsula, Russia. *European Journal of Mineralogy*, in press.
- Kunz, M. and Brown, I.D. (1995) Out-of-center distortions around octahedrally coordinated  $d^0$  transition metals. *Journal of Solid State Chemistry*, 112, 395–406.
- Kuznicki, S.M., Bell, V.A., Nair, S., Hillhouse, H.W., Jacobinas, R.M., Braunbarth, C.M., Toby, B.H., and Tsapatsis, M. (2001) A titanosilicate molecular sieve with adjustable pores for size-selective adsorption of molecules. *Nature*, 412, 720–724.
- Lamberti, C. (1999) Electron-hole reduced effective mass in monoatomic O-Ti-O-Ti-O quantum wires embedded in the siliceous crystalline matrix of ETS-10. *Microporous and Mesoporous Materials*, 30, 155–163.
- Liebau, F. (2003) Ordered microporous and mesoporous materials with inorganic hosts: definitions of terms, formula notation, and systematic classification. *Microporous and Mesoporous Materials*, 58, 15–72.
- Mer'kov, A.N., Bussen, I.V., Goiko, E.A., Kul'chitskaya, E.A., Men'shikov, Yu.P., and Nedorezova, A.P. (1973) Raite and zorite, new minerals from the Lovozero tundra. *Zapiski Vsesoyuznogo Mineralogicheskogo Obshchestva*, 102, 54–62.
- Merlino, S., Bonaccorsi, E., and Armbuster, T. (1999) Tobermorites: their real structure and order-disorder (OD) character. *American Mineralogist*, 84, 1613–1621.
- — — (2001) The real structure of tobermorite 11 Å: normal and anomalous forms, OD character and polytypic modifications. *European Journal of Mineralogy*, 13, 577–590.
- Nespolo, M. and Ferraris, G. (2000) Twinning by syngonic and metric merohedry. Analysis, classification and effects on the diffraction pattern. *Zeitschrift für Kristallographie*, 215, 77–81.
- Rastsvetaeva, R.K. (1986) Crystal structure of lomonosovite from the Lovozero region. *Soviet Physics Crystallography*, 31, 633–636.
- Rocha, J. and Anderson, M.W. (2000) Microporous titanosilicates and other novel mixed octahedral-tetrahedral framework oxides. *European Journal of Inorganic Chemistry*, 2000, 801–818.
- Sandomirskii, P.A. and Belov, N.V. (1979) The OD structure of zorite. *Soviet Physics Crystallography*, 24, 686–693.
- Wise, W.S., Pabst, A., and Hinthorne, J.R. (1977) Jonesite, a new mineral from the Benitoite Gem Mine, San Benito County, California. *Mineralogical Record*, 8, 453–456.
- Zecchina, A., Llabres i Xamena, F.X., Paze, C., Turnes Palomino, G., Bordiga, S., and Otero Arean, C. (2001) Alkyne polymerization on the titanosilicate molecular sieve ETS-10. *Physical Chemistry Chemical Physics*, 3, 1228–1231.

MANUSCRIPT RECEIVED MAY 26, 2003

MANUSCRIPT ACCEPTED JUNE 10, 2003

MANUSCRIPT HANDLED BY SIMONA QUARTIERI